

**Simulation of
solar-cycle response
in tropical total
column ozone**

K.-F. Li et al.

**Simulation of solar-cycle response in
tropical total column ozone using
SORCE irradiance**

K.-F. Li¹, X. Jiang², M.-C. Liang^{3,4,5}, and Y. L. Yung¹

¹Division of Geological and Planetary Sciences, California Institute of Technology, Pasadena, CA, USA

²Department of Earth and Atmospheric Sciences, University of Houston, Houston, Texas, USA

³Research Centre for Environmental Changes, Academia Sinica, Taipei, Taiwan

⁴Institute of Astronomy and Astrophysics, Academia Sinica, Taipei, Taiwan

⁵Graduate Institute of Astronomy, National Central University, Jhongli City, Taiwan

Received: 4 December 2011 – Accepted: 27 December 2011 – Published: 19 January 2012

Correspondence to: K.-F. Li (kfl@gps.caltech.edu)

Published by Copernicus Publications on behalf of the European Geosciences Union.

Title Page

Abstract

Introduction

Conclusions

References

Tables

Figures

⏪

⏩

◀

▶

Back

Close

Full Screen / Esc

Printer-friendly Version

Interactive Discussion

Abstract

Total column ozone (X_{O_3}) abundance in Earth's atmosphere is intimately related to atmospheric chemistry and dynamics. Understanding the solar-cycle modulations of X_{O_3} helps distinguish anthropogenic perturbations from natural variability during the ozone recovery. Here, the solar-cycle signal of tropical X_{O_3} in the Whole Atmosphere Community Climate Model (WACCM) model has been examined using solar spectral irradiance (SSI) estimated from the Naval Research Laboratory (NRL) solar model and that from recent satellite measurements observed by the Solar Radiation and Climate Experiment (SORCE). Four experiments have been conducted with NRL/SORCE SSI and climatological/realistic sea surface temperatures and ice, and all other variability is fixed. In the tropical region 24°S – 24°N , using the SORCE SSI as a model input leads to a solar-cycle response of $\sim 5.4\text{ DU}/100F_{10.7}$, which is ~ 2 times of that obtained using NRL SSI. The results are slightly different in the presence of El Niño/Southern Oscillation (ENSO) when realistic SST/ice is used, but these differences are within the regression uncertainty of $\sim 0.6\text{ DU}/100F_{10.7}$. The solar-cycle responses simulated using SORCE SSI agree with those obtained from the merged TOMS/SBUV satellite observations. Using NRL SSI as a model input results in solar-cycle responses that are closer to the ground-based observations, although the accuracy of the latter is limited by the number of stations in the tropics. In all model experiments, the tropical distribution of the solar-cycle response is constant to within $\sim 0.5\text{ DU}/100F_{10.7}$, which is of the same order as the regression uncertainty. The spatial structures of the regression uncertainty are shown to be correlated with ENSO in the Pacific region. The solar-cycle response obtained using SORCE SSI implies a maximum change in lower stratospheric temperature of $\sim 0.8\text{ K}$. This may lead to significant impacts on the model solar-cycle responses in atmospheric circulation, precipitation and other hydrological variables that are important for the climate change.

Simulation of solar-cycle response in tropical total column ozone

K.-F. Li et al.

Title Page

Abstract

Introduction

Conclusions

References

Tables

Figures



Back

Close

Full Screen / Esc

Printer-friendly Version

Interactive Discussion



1 Introduction

The solar-cycle variability has long been believed to have impacts on Earth's climate (Herschel, 1801). Of only $\sim 0.1\%$ peak-to-trough variations in the total solar irradiance, the 11-yr solar-cycle variability is most noticeable in the ultraviolet (UV) regions. The variability ranges from $\sim 70\%$ at the hydrogen Lyman- α transition line (121.57 nm) to $\sim 10\%$ in 200–300 nm (Marsh et al., 2007). Therefore, any impacts on Earth's climate are likely to be linked through upper atmospheric regions where UV is absorbed. For example, Meehl et al. (2009) suggests a top-down mechanism, wherein the production of tropical stratospheric ozone (O_3) is enhanced during a solar-cycle maximum through the absorption of anomalously high UV radiation by the oxygen molecule in the Schumann-Runge band (150–240 nm), which in turn leads to an enhanced UV absorption by ozone in the Hartley band (240–310 nm) (Brasseur and Solomon, 1984; Herzberg, 1965). The different heating of the stratosphere as a function of latitude due to these absorption processes may modify the tropospheric circulation, leading to changes in the hydrological cycle (van Loon et al., 2007; Meehl et al., 2009). Since the solar irradiance is strongest over the equatorial region and the stratospheric O_3 is produced mainly in the tropical area, we expect maximum solar-cycle modulation in the tropical O_3 (Camp et al., 2003). Such solar-cycle modulation can also be transported to higher latitudes by the Brewer-Dobson circulation in the middle atmosphere (Brasseur, 1993; Ineson et al., 2011).

The total column O_3 (hereafter denoted by X_{O_3}) has been measured from space since 1978 by the Total Ozone Mapping Spectrometer (TOMS) and the Solar Backscatter Ultraviolet (SBUV) aboard a series of satellite platforms (Stolarski et al., 2006), and the Ozone Monitoring Instrument (OMI) aboard Aura (Levelt et al., 2006). These observations merged together provide the longest satellite record of X_{O_3} for exploring interannual and decadal variabilities. There are also long-term ground-based measurements of O_3 but they are sparse in both space and time.

Simulation of solar-cycle response in tropical total column ozone

K.-F. Li et al.

Title Page

Abstract

Introduction

Conclusions

References

Tables

Figures



Back

Close

Full Screen / Esc

Printer-friendly Version

Interactive Discussion



with increasing latitude, atmospheric dynamics may interact with the solar-cycle modulations and make the interpretation difficult in the extratropics for both model and observational results (see, e.g., Jiang et al., 2008a, b), which is out of the scope of this work.

2 Model setup

WACCM is a global atmospheric model with fully coupled chemistry, radiation and dynamics extending from the surface to the thermosphere based on version 3 of the Community Atmosphere Model (CAM3) (Marsh et al., 2007). It has a horizontal resolution of 5° longitude \times 4° latitude. There is a resolved stratosphere with fully interactive ozone chemistry that can respond to the UV part of the solar forcing. This model is one of the participants of the CCMVal activity and has been employed to project the ozone trend in the 21st century (Oman et al., 2010). The version that we use does not have an internal mechanism for generating quasi-biennial oscillations (QBOs), although there have been efforts where relaxation methods have been employed to externally impose the QBO in the simulations (Matthes et al., 2010). A parametrized gravity wave drag has been used to drive the Brewer-Dobson circulation (Richter et al., 2010).

We shall explore the impact of two sets of SSI inputs derived from NRL solar model and from the recent SORCE measurements on the model X_{O_3} . The spectral variability between 115–400 nm for 2004–2007 depicted by these two spectral datasets as well as their implications for stratospheric chemistry have been studied in details by several groups (Cahalan et al., 2010; Haigh et al., 2010; Merkel et al., 2011). Their model results have also been compared against vertically resolved satellite data that are available during the same period. In order to simulate the modulation of a full solar cycle, we extrapolate the SORCE measurements back to the last solar maximum in 2002 using the Magnesium-II core-to-wing ratio (Mg-II c/w) index. The extrapolation procedure has been described in details by Wang et al. (2012). In this work, wavelengths below 240 nm are derived from the spectral measurements by the Solar Stellar Irradiance Comparison Experiment (SOLSTICE) aboard SORCE, whereas wavelengths above

Simulation of solar-cycle response in tropical total column ozone

K.-F. Li et al.

Title Page

Abstract

Introduction

Conclusions

References

Tables

Figures



Back

Close

Full Screen / Esc

Printer-friendly Version

Interactive Discussion



240 nm are derived from the measurements by the Spectral Irradiance Monitor (SIM) aboard SORCE. The 2002/2007 SSI ratios derived from the two spectral datasets are incorporated into the model.

In the WACCM model, $F_{10.7}$ serves as a proxy for the solar cycle. The corresponding variability in the UV region is characterized by the fractional changes from the (extrapolated) solar maximum of Solar Cycle 23 in 2002 to the solar minimum in 2007. The spectral variability is assumed to follow the phase of $F_{10.7}$. The model also requires other solar quantities including the sunspot number and the daily planetary K and a indices. The stratospheric chlorine has been fixed in the simulations.

The WACCM model is run with the atmospheric module only so that there is no dynamical coupling between the atmosphere and the ocean. The oceanic variability is prescribed by putting in the sea surface temperatures and ice (SST/ice) as boundary conditions. In order to isolate the effects due to the solar cycle, we run the model with monthly climatological SST/ice (experiments A & C). This reduces the interaction or aliasing with oceanic long-term modes such as the El Niño/Southern Oscillation (ENSO). To evaluate the effects due to the natural oceanic modes, we conduct another set of simulations with realistic SST/ice (Hurrell et al., 2008) (experiments B & D). Besides the ENSO, the realistic SST/ice also includes a tiny solar-cycle variability of ~ 0.1 K peak-to-trough (Zhou and Tung, 2010). Therefore, such prescription may mimic a coupled atmosphere-ocean system and provide an estimate of the bottom-up effect on the ozone column abundance due to the solar cycle (Meehl et al., 2009). Lastly, in order to estimate the relative contribution of the simulated solar response due to that tiny solar-cycle variability in the SST/ice, we conduct a control run with realistic SST/ice where the solar constant is time-independent (experiment E).

The model was run from January 1960 to November 2009. To avoid analyzing transient signals, we omit the first 10 yr of simulations and analyze data only from January 1970 to the end of the simulations. We summarize and define the assumptions for these experimental setups in Table 1.

Simulation of solar-cycle response in tropical total column ozone

K.-F. Li et al.

Title Page

Abstract

Introduction

Conclusions

References

Tables

Figures



Back

Close

Full Screen / Esc

Printer-friendly Version

Interactive Discussion

3 Multiple linear regression

We follow the procedure for multiple linear regression as described in Randel and Cobb (1994). The simulated X_{O_3} time series are first deseasonalized to obtain monthly anomalies, to which a smoothing 1-2-1 filter is then applied. Subsequently, the solar-cycle modulation is retrieved using a regression model delineated in Li et al. (2008):

$$\begin{aligned} X_{O_3}(t) = & \alpha(t) \cdot t \\ & + \beta(t) \cdot F_{10.7}(t) \\ & + \gamma_1(t) \cdot QBO_1(t) + \gamma_2(t) \cdot QBO_2(t) \\ & + \varepsilon(t) \cdot ENSO(t) \\ & + \text{residual} \end{aligned} \quad (1)$$

where X_{O_3} represents the monthly anomaly of total column ozone, $F_{10.7}(t)$ is the 10.7-cm solar radio flux. Although QBO is not simulated in WACCM, we keep the QBO terms so that the model results can be consistently compared with observations (Randel and Wu, 2007). $QBO_1(t)$ and $QBO_2(t)$ are a pair of QBO indices derived from stratospheric zonal winds over Singapore (Wallace et al., 1993). Using these two QBO indices together could capture the downward propagation of the QBO in the equatorial stratospheric wind (Randel and Wu, 1996; Li et al., 2008). $ENSO(t)$ is the ENSO index described by the Multivariate ENSO Index (MEI) (Wolter and Timlin, 2011). Aerosol effects are considered to be negligible (Randel and Wu, 2007). The time-varying coefficients α , β , γ_1 , γ_2 , and ε are the sum of a constant term and annual harmonics:

$$\alpha(t) = A_1 + A_2 \cos \omega t + A_3 \sin \omega t \quad (2)$$

where $\omega = 2\pi/12$ months. Therefore a total of 15 parameters are retrieved from the analysis. The uncertainties of the above 5 coefficients are related to the 15 retrieved parameters via the following relation (Bevington and Robinson, 1992):

$$\begin{aligned} \text{var}[\alpha(t)] = & \text{var}(A_1) + \text{var}(A_2) \cos^2 \omega t + \text{var}(A_3) \sin^2 \omega t \\ & + 2 \times [\text{cov}(A_1, A_2) \cos \omega t + \text{cov}(A_1, A_3) \sin \omega t + \text{cov}(A_2, A_3) \cos \omega t \sin \omega t] \end{aligned} \quad (3)$$

Simulation of solar-cycle response in tropical total column ozone

K.-F. Li et al.

Title Page

Abstract

Introduction

Conclusions

References

Tables

Figures

⏪

⏩

◀

▶

Back

Close

Full Screen / Esc

Printer-friendly Version

Interactive Discussion



The time-averaged coefficients and the corresponding uncertainties are thus given by

$$\overline{\alpha(t)} = A_1 \quad (4)$$

$$\overline{\text{var}[\alpha(t)]} = \text{var}(A_1) + \frac{1}{2} [\text{var}(A_2) + \text{var}(A_3)] \quad (5)$$

where the overbar denotes temporal averages.

4 Results

In this section, we first establish the solar-cycle responses in the tropical averages. The relative importance of the modulations due to the solar cycle and the ENSO are studied through the regression coefficients and their uncertainties. Then the latitudinal patterns are presented and are compared with observations derived in previous studies. Finally, the spatial patterns in the tropical area are also discussed.

4.1 Tropical averages and regression coefficients

Figure 1 shows the simulated monthly mean of tropical X_{O_3} averaged over 24°S – 24°N . Latitudinal area weighting has been applied. The color code for the time series corresponds to those of the average contour shown in Fig. 3; see below and Table 1. Regression is then applied to the equatorial average using Eq. (1). The $F_{10.7}$ index multiplied by the time-averaged fitting coefficients, $\bar{\beta}F_{10.7}(t)$, of the respective experiments are shown as black lines.

In all experiments, the regression uncertainties (2σ) of $\bar{\beta}$ are about 0.5–0.6 DU/100 $F_{10.7}$ (Table 2). The regressed coefficients $\bar{\gamma}_1$ and $\bar{\gamma}_2$ for QBO are statistically insignificant, as expected. The regressed coefficients $\bar{\alpha}$ for the trends are insignificant (0.03 DU/yr) for those runs with climatological SST/ice (experiments A and C). On the other hand, there are non-zero trends for experiments B and E with realistic SST/ice inputs. Part of them may be due to the trends in the realistic SST/ice in the last three

Simulation of solar-cycle response in tropical total column ozone

K.-F. Li et al.

Title Page

Abstract

Introduction

Conclusions

References

Tables

Figures

⏪

⏩

◀

▶

Back

Close

Full Screen / Esc

Printer-friendly Version

Interactive Discussion



decades ($\sim 0.3\text{--}0.6\text{ K}$) over the tropics (Keihm et al., 2009). We note that the regressed coefficients remain statistically the same when the linear trend is absent in Eq. (1). Therefore, we shall not discuss $\bar{\alpha}$ further. Finally, the regressed coefficients $\bar{\epsilon}$ for ENSO are $-1.17 \pm 0.26\text{ DU/MEI}$, $-1.36 \pm 0.30\text{ DU/MEI}$, and $-1.43 \pm 0.29\text{ DU/MEI}$ for experiments B, D, and E, respectively, and these values are mutually consistent within uncertainties. The anti-correlation implies that X_{O_3} is primarily controlled by the vertical motion of the tropopause related to the ENSO modulations, likely through the strengthening/weakening of Brewer-Dobson circulation over the anomalously warm/cool sea surface (Camp et al., 2003). Another set of regression coefficients has been obtained by omitting the ENSO term for experiments A and C. The resultant values of $\bar{\beta}$ remain statistically the same, but the uncertainties are slightly larger ($0.7\text{ DU}/100F_{10.7}$).

In experiments A and B where NRL SSI is used, the regressed solar-cycle responses $\bar{\beta}$ are $3.11\text{ DU}/100F_{10.7}$ and $2.67\text{ DU}/100F_{10.7}$, respectively, but these values are again mutually consistent within uncertainties. The decrease in the regressed response in experiment B is likely due to modulations by the ENSO signal. Such modulation is most notable during the simulation years 1973–1976, when there were strong and prolonged La Niña events (indicated in Fig. 1 by the green bars) which enhances X_{O_3} during the solar minimum. Similarly, in experiments C and D where SORCE SSI is used, the fitted solar-cycle responses $\bar{\beta}$ are $5.46\text{ DU}/100F_{10.7}$ and $5.44\text{ DU}/100F_{10.7}$ respectively, and they are mutually consistent within uncertainties ($\sim 0.6\text{ DU}/100F_{10.7}$). Therefore, the solar-cycle response in X_{O_3} obtained using SORCE SSI is almost two times that obtained using NRL SSI. This is because of an enhanced production of stratospheric O_3 at wavelengths below 240 nm as revealed in the SORCE SSI. Furthermore, the difference in the solar-cycle responses obtained using two different SSI settings is statistically significant. The solar-cycle response obtained using SORCE SSI is close to the observed value over $24^\circ\text{ S}\text{--}24^\circ\text{ N}$, which is $5.54\text{ DU}/100F_{10.7}$ (Randel and Wu, 2007).

When the solar constant is fixed but the realistic SST/ice is employed in experiment E, the regressed solar response $\bar{\beta}$ is only $-0.27\text{ DU}/100F_{10.7}$ and is much smaller

Simulation of solar-cycle response in tropical total column ozone

K.-F. Li et al.

Title Page

Abstract

Introduction

Conclusions

References

Tables

Figures

⏪

⏩

◀

▶

Back

Close

Full Screen / Esc

Printer-friendly Version

Interactive Discussion

than the regression uncertainty $0.59 \text{ DU}/100F_{10.7}$. Therefore we conclude that even if there is a tiny modulation due to the solar-cycle signal in the realistic SST/ice, the simulated response would not be discernible against the natural variability through our regression model.

5 4.2 Latitudinal patterns and the equatorial paradox

Figure 2 shows the latitudinal patterns of the time-averaged solar-cycle response between 24° S – 24° N . To obtain these results, the regression analysis has been applied to individual zonal averages at different latitudes. The regression uncertainty (2σ) is roughly equal to the error bar shown in Fig. 2, which is $\sim 0.6 \text{ DU}/100F_{10.7}$. Also shown are the solar-cycle response derived from the TOMS/SBUV data (gray shade), the ground-based measurements made using Dobson and Brewer spectrophotometer, and the filter ozonometer (dashed line) (Fioletov et al., 2002). These data are extracted from Fig. 6 of Randel and Wu (2007).

For experiments A and B with NRL SSI input, the solar-cycle responses are $\sim 3 \text{ DU}/100F_{10.7}$. This agrees with those derived from the ground-based measurements (Austin et al., 2008). In contrast, experiments C and D with SORCE SSI input produce solar-cycle responses of $\sim 5.4 \text{ DU}/100F_{10.7}$, about a factor of 2 larger than those in experiments A and B, and they agree with those derived from TOMS/SBUV.

In all experiments with solar-cycle forcings, the values of $\bar{\beta}$ corresponding to the WACCM runs are relatively constant over the tropics, consistent with previous modeling studies (Brasseur, 1993; Lee and Smith, 2003; Tourpali et al., 2003; Egorova et al., 2004; Austin et al., 2008). In contrast, the latitudinal patterns in TOMS/SBUV and ground-based measurements are slightly lower at the equatorial region below 20° N/S . Previous simulations by Lee and Smith (2003) and McCormack et al. (2007) using 2-D chemical transport models with solar-cycle forcings only predict a constant response in the equatorial region. When QBO is included in the simulations, they both found that the solar-cycle response near the equator becomes lower than that in the mid-latitudes. Nonetheless, they drew totally different conclusions: Lee et al. assert that

Simulation of solar-cycle response in tropical total column ozone

K.-F. Li et al.

Title Page

Abstract

Introduction

Conclusions

References

Tables

Figures

⏪

⏩

◀

▶

Back

Close

Full Screen / Esc

Printer-friendly Version

Interactive Discussion



regression uncertainties have a lot more structures when the realistic SST/ice are included, especially over the Cold Tongue and the Warm Pool regions (Fig. 4). In the subtropics, the uncertainties are generally $\sim 1 \text{ DU}/100F_{10.7}$ and can be greater than 1.3 DU in the Northern Hemisphere. In the Central Pacific, the minimum uncertainties can be as low as $0.4 \text{ DU}/100F_{10.7}$ for experiments A and C; they are slightly higher ($\sim 0.6 \text{ DU}/100F_{10.7}$) for experiments B and D. These clearly show the effects of ENSO. It also becomes obvious when one examines the spatial pattern of the regressed coefficients $\bar{\epsilon}$ related to ENSO, shown in Fig. 5 only for experiments B, D, and E. The coefficients $\bar{\epsilon}$ are negative all over the tropics. The strongest ENSO modulations of $\sim 3 \text{ DU}/\text{MEI}$ are found over the Northern and Southern Eastern Pacific. The modulations are almost zero over the Warm Pool region, demonstrating the dipole structures of the ENSO effects. These spatial patterns are similar to the fourth EOF obtained by Camp et al. (2003).

As in previous sections, the regressed solar response of $-0.3 \text{ DU}/100F_{10.7}$ in experiment E is insignificant compared to the regression uncertainty shown in Fig. 4, implying that the modulation due to the solar-cycle signal in the realistic SST/ice is tiny. We also point out that the regression uncertainty seems to be independent of the input solar flux and SST/ice. Rather, it depends largely on the internal variability of the model.

For comparison, we apply the same regression analysis to the monthly-averaged TOMS/SBUV data (Randel and Wu, 2007; Stolarski et al., 2006). The linear trend $\alpha(t) \cdot t$ in Eq. (1) is replaced by $\alpha(t) \cdot \text{EESC}(t)$, where EESC is the equivalent effective stratospheric chlorine (WMO, 2007, chapter 1). The results are shown in the bottom panels of Figs. 3 and 4. We note that the interpretation of these spatial structures may be cautionary because the ozone columns are observed only twice a day (one during daytime and the other during nighttime) from space. Planetary wave activities of short time scales (e.g. diurnally to daily) may have not been efficiently suppressed by the monthly averages. The solar-cycle response shows a strong latitudinal variation at all longitudes. It attains the lowest values ($3\text{--}4 \text{ DU}/100F_{10.7}$) over the Indo-Pacific region. Over the subtropics, the average response is $\sim 6 \text{ DU}/100F_{10.7}$ and it can be

**Simulation of
solar-cycle response
in tropical total
column ozone**

K.-F. Li et al.

Title Page

Abstract

Introduction

Conclusions

References

Tables

Figures

⏪

⏩

◀

▶

Back

Close

Full Screen / Esc

Printer-friendly Version

Interactive Discussion

more than $8 \text{ DU}/100F_{10.7}$ over Northern Pacific. Due to short-term natural variability, including those planetary waves mentioned above, the regression uncertainty is much higher than those obtained from WACCM. In general, the uncertainty is lower ($\sim 1 \text{ DU}/100F_{10.7}$) in the tropics but it can be as high as $\sim 2 \text{ DU}/100F_{10.7}$ over convective regions such as the Warm Pool; it is also higher ($\sim 2 \text{ DU}/100F_{10.7}$) over the subtropics and can be more than $\sim 3 \text{ DU}/100F_{10.7}$ over Northern Pacific. We note that both model and observations are subject to larger uncertainties over the subtropics, likely because of the dynamical variability over those latitudes.

To conclude, the simulated solar-cycle response when SORCE SSI is used has roughly the same order-of-magnitude as those derived from TOMS/SBUV data. However, the observation shows more structures in the latitudinal pattern, which have not been simulated in the model.

5 Summary and discussions

This work extends the modeling studies of Haigh et al. (2010) and Merkel et al. (2011) for middle atmospheric O_3 concentrations. Our simulations were done with much longer periods (1960–2009) in attempt to minimize statistical uncertainties. The solar-cycle responses of total column ozone, X_{O_3} , over the tropics in the WACCM model were simulated using spectral solar variability in UV derived from a conventional model developed in NRL and that from the SORCE measurements. For SORCE where the measurements covers only from 2004 to 2010, a full Solar Cycle 23 has been extrapolated based on the Mg-II c/w index (Wang et al., 2012).

Using the (extrapolated) SORCE spectral UV data, the stimulated solar-cycle modulations in tropical X_{O_3} has a sensitivity $\sim 5.4 \text{ DU}/100F_{10.7}$ or $\sim 2\%/100F_{10.7}$. This agrees with the sensitivity observed by TOMS/SBUV, although TOMS/SBUV observations suggest a local minimum of $\sim 4.5 \pm 1.5 \text{ DU}/100F_{10.7}$ at the equator, which is not simulated in the model. This is about twice that obtained using NRL SSI. The reason is an enhanced production of stratospheric O_3 at wavelengths below 240 nm as revealed

Simulation of solar-cycle response in tropical total column ozone

K.-F. Li et al.

Title Page

Abstract

Introduction

Conclusions

References

Tables

Figures

⏪

⏩

◀

▶

Back

Close

Full Screen / Esc

Printer-friendly Version

Interactive Discussion



in the *SORCE* SSI. The inclusion of ENSO in the model runs does not statistically modify the simulated solar sensitivity. Such difference in the X_{O_3} solar-cycle sensitivity is likely to be applicable to other CCMVal models, although there may be some nonlinearity due to dynamical changes. Analogous simulations using other CCMVal models help evaluate the robustness of these changes in solar-cycle sensitivities (Swartz et al., 2011).

Multiple linear regression has been frequently used for examining solar-cycle modulations and other forcings in global ozone data as well as other atmospheric variables (Hood and Soukharev, 2006; Soukharev and Hood, 2006; Randel and Wu, 2007; Zhou and Tung, 2010). It is easy to implement but it also has to assume that the forcings are independent of each other and that the responses are linear. However, in reality these assumptions may not always hold. For example, Meehl et al. (2009) suggests that the net effect of increased solar insolation during solar maximum conditions may result in stronger trade winds in the tropical Pacific, which may also impact the Walker circulation and hence ENSO. It is thus important to consider the regression uncertainties when interpreting the results.

There have been debates whether inclusion of an ENSO index in the regression model would lead to statistically different outcomes of the regressed responses (Marsh and Garcia, 2007; Hood et al., 2010). When studying the potential impacts in our regression coefficients due to the presence of ENSO, we have used the same regression model on different simulations with and without ENSO forcings. This is slightly different from the work of Marsh and Garcia (2007), where they applied two different regression models with and without the ENSO term on the same simulation. Our results show that when ENSO is prescribed via the realistic SST/ice, the regressed solar response shows an ENSO-like spatial variation but the variation is not statistically significant against the regression uncertainty. Therefore, we are not able to conclude from the above simulations whether the ENSO modulation in model O_3 may interact with the solar cycle modulation. On the other hand, Zhou and Tung (2010) examined the solar-cycle modulation in a 150-yr record of global SST and found that the resultant solar response is

Simulation of solar-cycle response in tropical total column ozone

K.-F. Li et al.

[Title Page](#)[Abstract](#)[Introduction](#)[Conclusions](#)[References](#)[Tables](#)[Figures](#)[Back](#)[Close](#)[Full Screen / Esc](#)[Printer-friendly Version](#)[Interactive Discussion](#)

neither La Niña-like nor El Niño-like. Their conclusion emphasizes the use of long-term records for establishing a statistically robust signal. Therefore, a longer simulation up to a centennial time scale may be required to clarify the interaction between the ENSO and the solar cycle in model O₃.

5 The above arguments may also apply to the effects of QBO as discussed in previous sections, but our model does not have a prescribed/simulated QBO for verification. Kuai et al. (2009) has shown that QBO may interact with the solar cycle nonlinearly through wave-semiannual oscillation. This effect must be considered in future modeling studies.

10 The above results may lead to significant changes in model global circulations that have not been explored in this work. Lower stratospheric heating is enhanced due to increased UV absorption by the enhanced O₃. A modeling study by Haigh et al. (2005) suggests that the enhanced lower stratospheric heating during the solar maximum conditions tends to weaken and expand the tropical Hadley cells and shift the Ferrell cells poleward, even though there is no direct solar forcing at the tropopause. The total change in X_{O₃} due to the UV variability in Solar Cycle 23 estimated in this and previous studies (e.g. Randel and Wu, 2007) is about $5.4 \times 1.5 = 8.1$ DU (assuming a total change of 150 units in $F_{10.7}$). This suggests that a maximum change of 0.81 K in lower stratospheric temperature between 10–100 hPa (Jiang et al., 2008b) may be attributed to the solar cycle. This is larger than the observed values 0.5–0.7 K in the lower stratosphere derived from reanalysis data (see Fig. 1b of Frame and Gray, 2010). On the other hand, the expected change in lower stratospheric temperature if NRL flux is applied is 0.39 K, which is less than the observed value. Therefore, a revised calculation of the potential impacts to the solar-cycle related modulations in large-scale circulations, sea surface temperatures and their induced changes in precipitation in
25 a coupled ocean-atmosphere experiment is highly desirable.

Acknowledgement. The 10-cm solar radio flux, sunspot number and daily planetary K and a indices used in this study were obtained from ftp://ftp.ngdc.noaa.gov/STP/GEOMAGNETIC_DATA/INDICES/KP_AP/. The Multivariate ENSO Index was obtained from <http://www.esrl.noaa.gov>.

Simulation of solar-cycle response in tropical total column ozone

K.-F. Li et al.

Title Page

Abstract

Introduction

Conclusions

References

Tables

Figures



Back

Close

Full Screen / Esc

Printer-friendly Version

Interactive Discussion



gov/psd/enso/mei/. The merged TOMS/SBUV data were obtained from http://acdb-ext.gsfc.nasa.gov/Data_services/merged/data/. We thank Run-Lie Shia for reviewing the manuscript. We thank Tao Li at the University of Science and Technology of China for valuable discussions on the multiple regression analysis. This work was supported in part by NASA grant P1095255 to the California Institute of Technology and NSC grant 98-2111-M-001-014-MY3 to Academia Sinica.

References

- Austin, J., Tourpali, K., Rozanov, E., Akiyoshi, H., Bekki, S., Bodeker, G., Bruhl, C., Butchart, N., Chipperfield, M., Deushi, M., Fomichev, V. I., Giorgetta, M. A., Gray, L., Kodera, K., Lott, F., Manzini, E., Marsh, D., Matthes, K., Nagashima, T., Shibata, K., Stolarski, R. S., Struthers, H., and Tian, W.: Coupled chemistry climate model simulations of the solar cycle in ozone and temperature, *J. Geophys. Res.-Atmos.*, 113, D11306, doi:10.1029/2007JD009391, 2008.
- Bevington, P. R. and Robinson, D. K.: *Data Reduction and Error Analysis for the Physical Sciences*, 3rd ed., McGraw-Hill, New York, 336 pp., 1992.
- Brasseur, G.: The response of the Middle Atmosphere to long-term and short-term solar variability – a 2-dimensional model, *J. Geophys. Res.-Atmos.*, 98, 23079–23090, doi:10.1029/93JD02406, 1993.
- Brasseur, G. and Solomon, S.: *Aeronomy of the Middle Atmosphere: Chemistry and Physics of the Stratosphere and Mesosphere*, Springer, Dordrecht, 1984.
- Cahalan, R. F., Wen, G., Harder, J. W., and Pilewskie, P.: Temperature responses to spectral solar variability on decadal time scales, *Geophys. Res. Lett.*, 37, L07705, doi:10.1029/2009GL041898, 2010.
- Camp, C. D., Roulston, M. S., and Yung, Y. L.: Temporal and spatial patterns of the interannual variability of total ozone in the tropics, *J. Geophys. Res.-Atmos.*, 108, 4643, doi:10.1029/2001JD001504, 2003.
- Egorova, T., Rozanov, E., Manzini, E., Haberreiter, M., Schmutz, W., Zubov, V., and Peter, T.: Chemical and dynamical response to the 11-year variability of the solar irradiance simulated with a chemistry-climate model, *Geophys. Res. Lett.*, 31, L06119, doi:10.1029/2003GL019294, 2004.

Simulation of solar-cycle response in tropical total column ozone

K.-F. Li et al.

Title Page

Abstract

Introduction

Conclusions

References

Tables

Figures



Back

Close

Full Screen / Esc

Printer-friendly Version

Interactive Discussion



Simulation of solar-cycle response in tropical total column ozone

K.-F. Li et al.

[Title Page](#)
[Abstract](#)
[Introduction](#)
[Conclusions](#)
[References](#)
[Tables](#)
[Figures](#)




[Back](#)
[Close](#)
[Full Screen / Esc](#)
[Printer-friendly Version](#)
[Interactive Discussion](#)


- Fioletov, V. E., Bodeker, G. E., Miller, A. J., McPeters, R. D., and Stolarski, R.: Global and zonal total ozone variations estimated from ground-based and satellite measurements: 1964–2000, *J. Geophys. Res.-Atmos.*, 107, 4647, doi:10.1029/2001JD001350, 2002.
- Frame, T. H. A. and Gray, L. J.: The 11-yr solar cycle in ERA-40 data: an update to 2008, *J. Clim.*, 23, 2213–2222, doi:10.1175/2009JCLI3150.1, 2010.
- Haigh, J. D., Blackburn, M., and Day, R.: The response of tropospheric circulation to perturbations in lower-stratospheric temperature, *J. Clim.*, 18, 3672–3685, doi:10.1175/JCLI3472.1, 2005.
- Haigh, J. D., Winning, A. R., Toumi, R., and Harder, J. W.: An influence of solar spectral variations on radiative forcing of climate, *Nature*, 467, 696–699, doi:10.1038/nature09426, 2010.
- Herschel, F. W.: Observations tending to investigate the nature of the Sun, in order to find the causes or symptoms of its variable emission of light and heat; with remarks on the use that may possibly be drawn from solar observations, *Philos. Trans. R. Soc. London*, 91, 265–318, 1801.
- Herzberg, L.: Solar optical radiation and its role in upper atmospheric processes, in: *Physics of the Earth's Upper Atmosphere*, edited by: Hines, C. O., Paglis, I., Hartz, R., and Fejer, J. A., Prentice Hall, New Jersey, 31–45, 1965.
- Hood, L. L. and Soukharev, B. E.: Quasi-decadal variability of the tropical lower stratosphere: the role of extratropical wave forcing, *J. Atmos. Sci.*, 60, 2389–2403, doi:10.1175/1520-0469(2003)060<2389:QVOTTL>2.0.CO;2, 2003.
- Hood, L. L. and Soukharev, B. E.: Solar induced variations of odd nitrogen: Multiple regression analysis of UARS HALOE data, *Geophys. Res. Lett.*, 33, L22805, doi:10.1029/2006GL028122, 2006.
- Hood, L. L., Soukharev, B. E., and McCormack, J. P.: Decadal variability of the tropical stratosphere: Secondary influence of the El Niño-Southern Oscillation, *J. Geophys. Res.-Atmos.*, 115, D11113, doi:10.1029/2009JD012291, 2010.
- Hurrell, J. W., Hack, J. J., Shea, D., Caron, J. M., and Rosinski, J.: A new sea surface temperature and sea ice boundary dataset for the Community Atmosphere Model, *J. Clim.*, 21, 5145–5153, doi:10.1175/2008jcli2292.1, 2008.
- Ineson, S., Scaife, A. A., Knight, J. R., Manners, J. C., Dunstone, N. J., Gray, L. J., and Haigh, J. D.: Solar forcing of winter climate variability in the Northern Hemisphere, *Nature Geosci.*, 4, 753–757, doi:10.1038/ngeo1282, 2011.
- Jiang, X., Pawson, S., Camp, C. D., Nielsen, J. E., Shia, R. L., Liao, T., Limpasuvan, V., and

Simulation of solar-cycle response in tropical total column ozone

K.-F. Li et al.

[Title Page](#)
[Abstract](#)
[Introduction](#)
[Conclusions](#)
[References](#)
[Tables](#)
[Figures](#)




[Back](#)
[Close](#)
[Full Screen / Esc](#)
[Printer-friendly Version](#)
[Interactive Discussion](#)

- Yung, Y. L.: Interannual variability and trends of extratropical ozone. Part I: Northern Hemisphere, *J. Atmos. Sci.*, 65, 3013–3029, doi:10.1175/2008JAS2665.1, 2008a.
- Jiang, X., Pawson, S., Camp, C. D., Nielsen, J. E., Shia, R. L., Liao, T., Limpasuvan, V., and Yung, Y. L.: Interannual variability and trends of extratropical ozone. Part II: Southern Hemisphere, *J. Atmos. Sci.*, 65, 3030–3041, doi:10.1175/2008JAS2793.1, 2008b.
- Keihm, S., Brown, S., Teixeira, J., Desai, S., Lu, W., Fetzer, E., Ruf, C., Huang, X. L., and Yung, Y.: Ocean water vapor and cloud liquid water trends from 1992 to 2005 TOPEX Microwave Radiometer data, *J. Geophys. Res.-Atmos.*, 114, D18101, doi:10.1029/2009JD012145, 2009.
- Kuai, L., Shia, R.-L., Jiang, X., Tung, K. K., and Yung, Y. L.: Modulation of the Period of the Quasi-Biennial Oscillation by the Solar Cycle, *J. Atmos. Sci.*, 66, 2418–2428, doi:10.1175/2009JAS2958.1, 2009.
- Lean, J.: Evolution of the sun's spectral irradiance since the Maunder Minimum, *Geophys. Res. Lett.*, 27, 2425–2428, doi:10.1029/2000GL000043, 2000.
- Lee, H. and Smith, A. K.: Simulation of the combined effects of solar cycle, quasi-biennial oscillation, and volcanic forcing on stratospheric ozone changes in recent decades, *J. Geophys. Res.-Atmos.*, 108, 4049, doi:10.1029/2001JD001503, 2003.
- Levelt, P. F., Hilsenrath, E., Leppelmeier, G. W., van den Oord, G. H. J., Bhartia, P. K., Tamminen, J., de Haan, J. F., and Veefkind, J. P.: Science objectives of the Ozone Monitoring Instrument, *IEEE T. Geosci. Remote*, 44, 1199–1208, doi:10.1109/tgrs.2006.872336, 2006.
- Li, T., Leblanc, T., and McDermid, I. S.: Interannual variations of middle atmospheric temperature as measured by the JPL lidar at Mauna Loa Observatory, Hawaii (19.5° N, 155.6° W), *J. Geophys. Res.-Atmos.*, 113, D14109, doi:10.1029/2007JD009764, 2008.
- Marsh, D. R. and Garcia, R. R.: Attribution of decadal variability in lower-stratospheric tropical ozone, *Geophys. Res. Lett.*, 34, L21807, doi:10.1029/2007GL030935, 2007.
- Marsh, D. R., Garcia, R. R., Kinnison, D. E., Boville, B. A., Sassi, F., Solomon, S. C., and Matthes, K.: Modeling the whole atmosphere response to solar cycle changes in radiative and geomagnetic forcing, *J. Geophys. Res.-Atmos.*, 112, D23306, doi:10.1029/2006JD008306, 2007.
- Matthes, K., Marsh, D. R., Garcia, R. R., Kinnison, D. E., Sassi, F., and Walters, S.: Role of the QBO in modulating the influence of the 11 year solar cycle on the atmosphere using constant forcings, *J. Geophys. Res.-Atmos.*, 115, D18110, doi:10.1029/2009JD013020, 2010.
- McCormack, J. P., Siskind, D. E., and Hood, L. L.: Solar-QBO interaction and its impact on

Simulation of solar-cycle response in tropical total column ozone

K.-F. Li et al.

[Title Page](#)
[Abstract](#)
[Introduction](#)
[Conclusions](#)
[References](#)
[Tables](#)
[Figures](#)




[Back](#)
[Close](#)
[Full Screen / Esc](#)
[Printer-friendly Version](#)
[Interactive Discussion](#)

- stratospheric ozone in a zonally averaged photochemical transport model of the middle atmosphere, *J. Geophys. Res.-Atmos.*, 112, D16109, doi:10.1029/2006JD008369, 2007.
- Meehl, G. A., Arblaster, J. M., Matthes, K., Sassi, F., and van Loon, H.: Amplifying the Pacific climate system response to a small 11-year solar cycle forcing, *Science*, 325, 1114–1118, doi:10.1126/science.1172872, 2009.
- Merkel, A. W., Harder, J. W., Marsh, D. R., Smith, A. K., Fontenla, J. M., and Woods, T. N.: The impact of solar spectral irradiance variability on middle atmospheric ozone, *Geophys. Res. Lett.*, 38, L13802, doi:10.1029/2011GL047561, 2011.
- Morgenstern, O., Giorgetta, M. A., Shibata, K., Eyring, V., Waugh, D. W., Shepherd, T. G., Akiyoshi, H., Austin, J., Baumgaertner, A. J. G., Bekki, S., Braesicke, P., Bruhl, C., Chipperfield, M. P., Cugnet, D., Dameris, M., Dhomse, S., Frith, S. M., Garny, H., Gettelman, A., Hardiman, S. C., Hegglin, M. I., Jockel, P., Kinnison, D. E., Lamarque, J. F., Mancini, E., Manzini, E., Marchand, M., Michou, M., Nakamura, T., Nielsen, J. E., Olivie, D., Pitari, G., Plummer, D. A., Rozanov, E., Scinocca, J. F., Smale, D., Teysedre, H., Toohey, M., Tian, W., and Yamashita, Y.: Review of the formulation of present-generation stratospheric chemistry-climate models and associated external forcings, *J. Geophys. Res.-Atmos.*, 115, D00M02, doi:10.1029/2009JD013728, 2010.
- Oman, L. D., Plummer, D. A., Waugh, D. W., Austin, J., Scinocca, J. F., Douglass, A. R., Salawitch, R. J., Canty, T., Akiyoshi, H., Bekki, S., Braesicke, P., Butchart, N., Chipperfield, M. P., Cugnet, D., Dhomse, S., Eyring, V., Frith, S., Hardiman, S. C., Kinnison, D. E., Lamarque, J. F., Mancini, E., Marchand, M., Michou, M., Morgenstern, O., Nakamura, T., Nielsen, J. E., Olivie, D., Pitari, G., Pyle, J., Rozanov, E., Shepherd, T. G., Shibata, K., Stolarski, R. S., Teysedre, H., Tian, W., Yamashita, Y., and Ziemke, J. R.: Multimodel assessment of the factors driving stratospheric ozone evolution over the 21st century, *J. Geophys. Res.-Atmos.*, 115, D24306, doi:10.1029/2010JD014362, 2010.
- Randel, W. J. and Cobb, J. B.: Coherent variations of monthly mean total ozone and lower stratospheric temperature, *J. Geophys. Res.-Atmos.*, 99, 5433–5447, 1994.
- Randel, W. J. and Wu, F.: Isolation of the ozone QBO in SAGE II data by singular-value decomposition, *J. Atmos. Sci.*, 53, 2546–2559, 1996.
- Randel, W. J. and Wu, F.: A stratospheric ozone profile data set for 1979–2005: Variability, trends, and comparisons with column ozone data, *J. Geophys. Res.-Atmos.*, 112, D06313, doi:10.1029/2006JD007339, 2007.
- Richter, J. H., Sassi, F., and Garcia, R. R.: Toward a physically based gravity wave

Simulation of solar-cycle response in tropical total column ozone

K.-F. Li et al.

[Title Page](#)
[Abstract](#)
[Introduction](#)
[Conclusions](#)
[References](#)
[Tables](#)
[Figures](#)




[Back](#)
[Close](#)
[Full Screen / Esc](#)
[Printer-friendly Version](#)
[Interactive Discussion](#)

source parameterization in a general circulation model, *J. Atmos. Sci.*, 67, 136–156, doi:10.1175/2009JAS3112.1, 2010.

Soukharev, B. E. and Hood, L. L.: Solar cycle variation of stratospheric ozone: Multiple regression analysis of long-term satellite data sets and comparisons with models, *J. Geophys. Res.-Atmos.*, 111, D20314, doi:10.1029/2006JD007107, 2006.

Stolarski, R. S., Douglass, A. R., Steenrod, S., and Pawson, S.: Trends in stratospheric ozone: lessons learned from a 3D chemical transport model, *J. Atmos. Sci.*, 63, 1028–1041, doi:10.1175/JAS3650.1, 2006.

Swartz, W. H., Stolarski, R. S., Oman, L. D., Fleming, E. L., and Jackman, C. H.: Middle atmosphere sensitivity to SSI solar cycle variations, in: *SORCE Science Team Meeting (September 2011)*, Sedona, AZ, 2011.

Tapping, K. F. and Detracey, B.: The origin of the 10.7 cm Flux, *Solar Phys.*, 127, 321–332, doi:10.1007/BF00152171, 1990.

Tourpali, K., Schuurmans, C. J. E., van Dorland, R., Steil, B., and Bruhl, C.: Stratospheric and tropospheric response to enhanced solar UV radiation: a model study, *Geophys. Res. Lett.*, 30, 1231, doi:10.1029/2002GL016650, 2003.

van Loon, H., Meehl, G. A., and Shea, D. J.: Coupled air-sea response to solar forcing in the Pacific region during northern winter, *J. Geophys. Res.-Atmos.*, 112, D02108, doi:10.1029/2006JD007378, 2007.

Wallace, J. M., Panetta, R. L., and Estberg, J.: Representation of the equatorial stratospheric quasi-biennial oscillation in EOF phase space, *J. Atmos. Sci.*, 50, 1751–1762, 1993.

Wang, S., Li, K.-F., Pongetti, T. J., Sander, S. P., Yung, Y. L., Liang, M.-C., Livesey, N. J., Santee, M. L., Harder, J. W., Snow, M., and Mills, F. P.: Atmospheric OH response to the 11-year solar cycle – could the gap between model and observations be filled by SORCE measurements?, *P. Natl. Acad. Sci. USA*, in review, 2012.

WMO: Scientific assessment of ozone depletion: 2006, *Global Ozone Research and Monitoring Project – Report No. 50*, World Meteorological Organization, Geneva, 2007.

Wolter, K. and Timlin, M. S.: El Niño/Southern Oscillation behaviour since 1871 as diagnosed in an extended multivariate ENSO index (MEI.ext), *Int. J. Climatol.*, 31, 1074–1087, doi:10.1002/joc.2336, 2011.

Zhou, J. and Tung, K.-K.: Solar cycles in 150 years of global sea surface temperature data, *J. Clim.*, 23, 3234–3248, doi:10.1175/2010JCLI3232.1, 2010.

Simulation of solar-cycle response in tropical total column ozone

K.-F. Li et al.

Table 1. Model simulations in this study and their identities. The color codes are assigned in accordance with the average contour colors shown in Fig. 3. Experiment A is run with solar spectral irradiance (SSI) from the Naval Research Laboratory (NRL) solar model and climatological sea surface temperature and ice (SST/ice). Experiment B is similar to experiment A except that the realistic SST/ice is used from 1960 to 2009. Similarly, experiment C is run with exoatmospheric SSI observed by the Solar Radiation and Climate Experiment (SORCE) and climatological SST/ice. Experiment D is similar to experiment C except that the realistic SST/ice is used. Experiment E is run with no solar-cycle variability in SSI and the realistic SST/ice is used.

Experiment	SSI			SST/ice		
	ID	NRL	SORCE	fixed	Climatological	Realistic
A		●			●	
B		●				●
C			●		●	
D			●			●
E				●		●

[Title Page](#)[Abstract](#)[Introduction](#)[Conclusions](#)[References](#)[Tables](#)[Figures](#)[⏪](#)[⏩](#)[◀](#)[▶](#)[Back](#)[Close](#)[Full Screen / Esc](#)[Printer-friendly Version](#)[Interactive Discussion](#)

Simulation of solar-cycle response in tropical total column ozone

K.-F. Li et al.

Table 2. Regression coefficients and corresponding uncertainties ($\pm 2\sigma$) described in Eqs. (1) and (2). They are temporally averaged according to Eqs. (3) and (4).

Experiment ID	$\bar{\alpha}$ (DU/yr)	$\bar{\beta}$ (DU/100F _{10.7})	$\bar{\gamma}_1$ (DU/QBO ₁)	$\bar{\gamma}_2$ (DU/QBO ₂)	$\bar{\varepsilon}$ (DU/MEI)
A	-0.02 ± 0.03	3.11 ± 0.56	0.04 ± 0.15	-0.13 ± 0.34	0.02 ± 0.27
B	-0.06 ± 0.03	2.67 ± 0.53	-0.17 ± 0.14	0.29 ± 0.33	-1.17 ± 0.26
C	0.00 ± 0.02	5.46 ± 0.47	0.00 ± 0.12	0.11 ± 0.29	0.14 ± 0.23
D	-0.02 ± 0.03	5.44 ± 0.61	0.08 ± 0.17	-0.15 ± 0.37	-1.36 ± 0.30
E	-0.05 ± 0.03	-0.27 ± 0.59	-0.11 ± 0.16	0.17 ± 0.36	-1.43 ± 0.29

[Title Page](#)
[Abstract](#)
[Introduction](#)
[Conclusions](#)
[References](#)
[Tables](#)
[Figures](#)
[⏪](#)
[⏩](#)
[◀](#)
[▶](#)
[Back](#)
[Close](#)
[Full Screen / Esc](#)
[Printer-friendly Version](#)
[Interactive Discussion](#)

Simulation of solar-cycle response in tropical total column ozone

K.-F. Li et al.

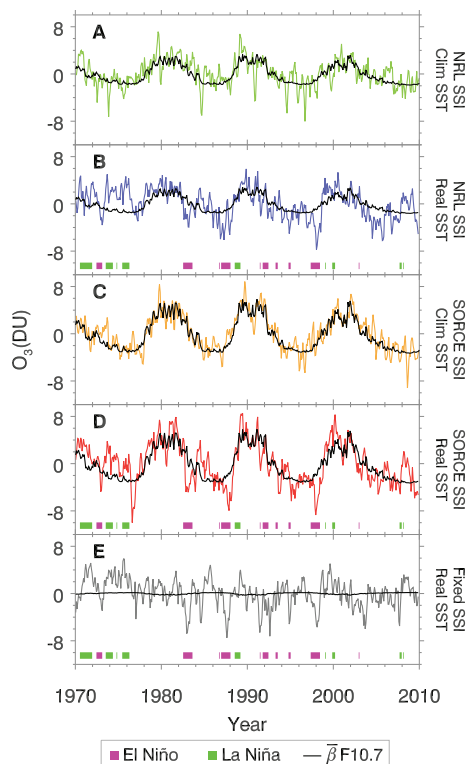


Fig. 1. Tropical averages of total column ozone X_{O_3} between $24^\circ N$ and $24^\circ S$ simulated by WACCM for four experimental setups identified in Table 1. The color codes are assigned in accordance with the average contour colors shown in Fig. 3. Overlaid black line is the regressed time series related to the solar variability described by the product $\bar{\beta}F_{10.7}$, where $\bar{\beta}$ is the time-averaged regression coefficient and $F_{10.7}$ is the 10.7-cm solar radio flux. Also shown by pink and green strokes are strong El Niño/La Niña events when the absolute values of the Multivariate El Niño/Southern Oscillation Index (MEI) are greater than 1.

Title Page

Abstract Introduction

Conclusions References

Tables Figures

◀ ▶

◀ ▶

Back Close

Full Screen / Esc

Printer-friendly Version

Interactive Discussion



Simulation of solar-cycle response in tropical total column ozone

K.-F. Li et al.

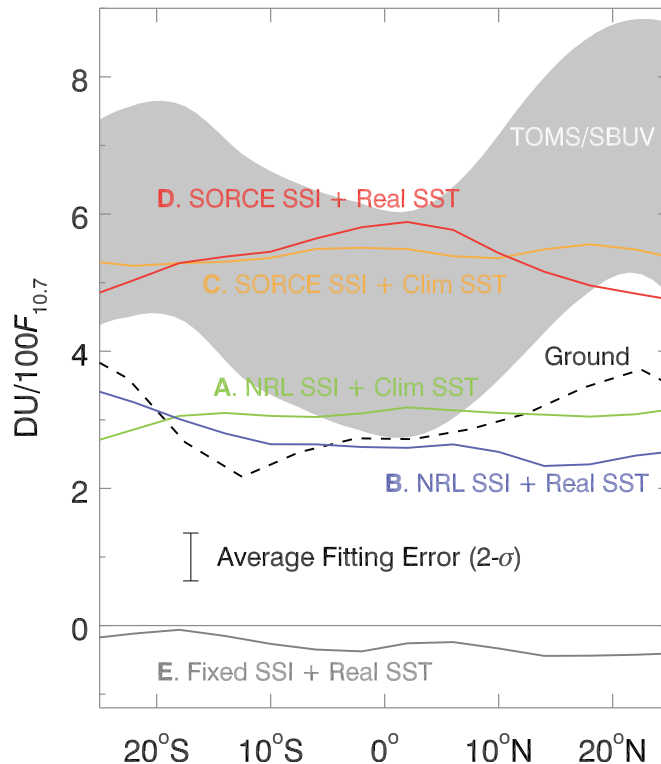


Fig. 2. Values of $\bar{\beta}$ as a function of latitudes for four experiments identified in Table 1. The color codes are assigned in accordance with the average contour colors shown in Fig. 3. Also shown in gray shade is the solar-cycle sensitivity of X_{O_3} derived from satellite measurements by the Total Ozone Mapping Spectrometer (TOMS) merged with the Solar Backscatter Ultraviolet (SBUV). The dashed line is the corresponding sensitivity derived from ground-based measurements. Both data of TOMS/SBUV and ground-based measurements are extracted from Fig. 6 of Randel and Wu (2007). The error bar shows the average regression error, which is $0.6 \text{ DU}/100F_{10.7} (2\sigma)$.

[Title Page](#)
[Abstract](#)
[Introduction](#)
[Conclusions](#)
[References](#)
[Tables](#)
[Figures](#)
[◀](#)
[▶](#)
[◀](#)
[▶](#)
[Back](#)
[Close](#)
[Full Screen / Esc](#)
[Printer-friendly Version](#)
[Interactive Discussion](#)

Simulation of solar-cycle response in tropical total column ozone

K.-F. Li et al.

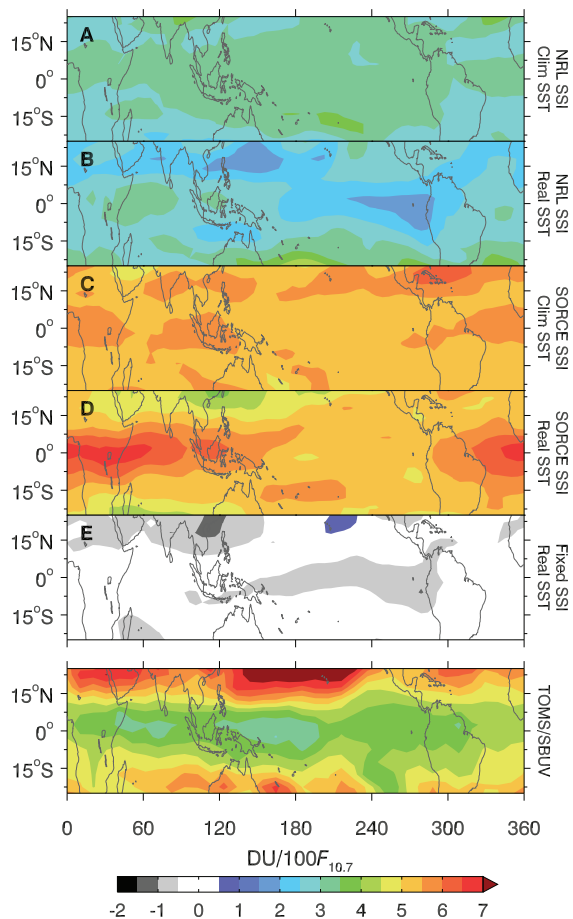


Fig. 3. Time-averaged regressed coefficients $\bar{\beta}$ for all experiments in the tropics. The multiple linear regression is applied to all individual grid points. The corresponding values derived from TOMS/SBUV are shown at the bottom.

Title Page

Abstract

Introduction

Conclusions

References

Tables

Figures

◀

▶

◀

▶

Back

Close

Full Screen / Esc

Printer-friendly Version

Interactive Discussion

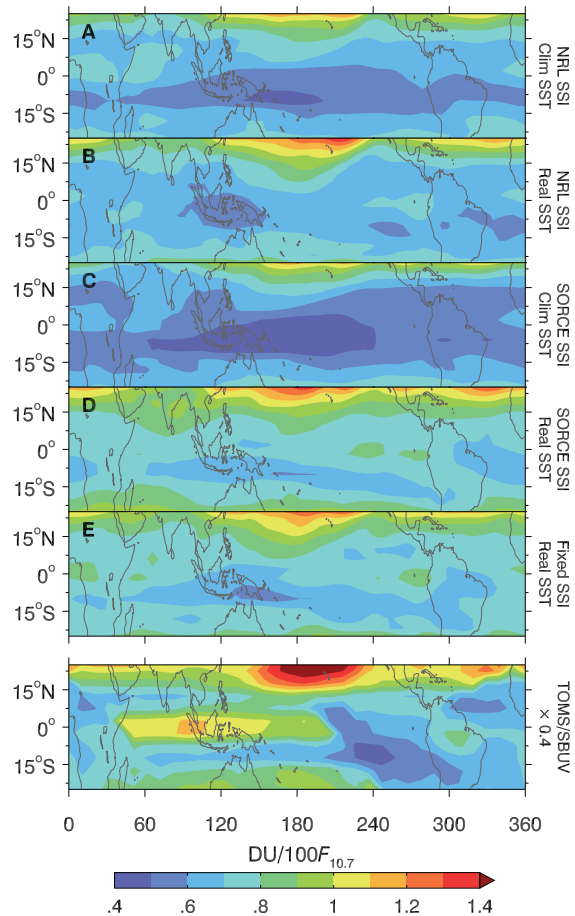


Fig. 4. Same as Fig. 3 except for the uncertainty (2σ) of the regressed coefficient, $\text{var}\bar{\beta}$, on individual model grid points. The uncertainty for TOMS/SBUV has been scaled by a factor of 0.4.

Simulation of solar-cycle response in tropical total column ozone

K.-F. Li et al.

Title Page

Abstract Introduction

Conclusions References

Tables Figures

◀ ▶

◀ ▶

Back Close

Full Screen / Esc

Printer-friendly Version

Interactive Discussion



**Simulation of
solar-cycle response
in tropical total
column ozone**

K.-F. Li et al.

Title Page

Abstract

Introduction

Conclusions

References

Tables

Figures

◀

▶

◀

▶

Back

Close

Full Screen / Esc

Printer-friendly Version

Interactive Discussion

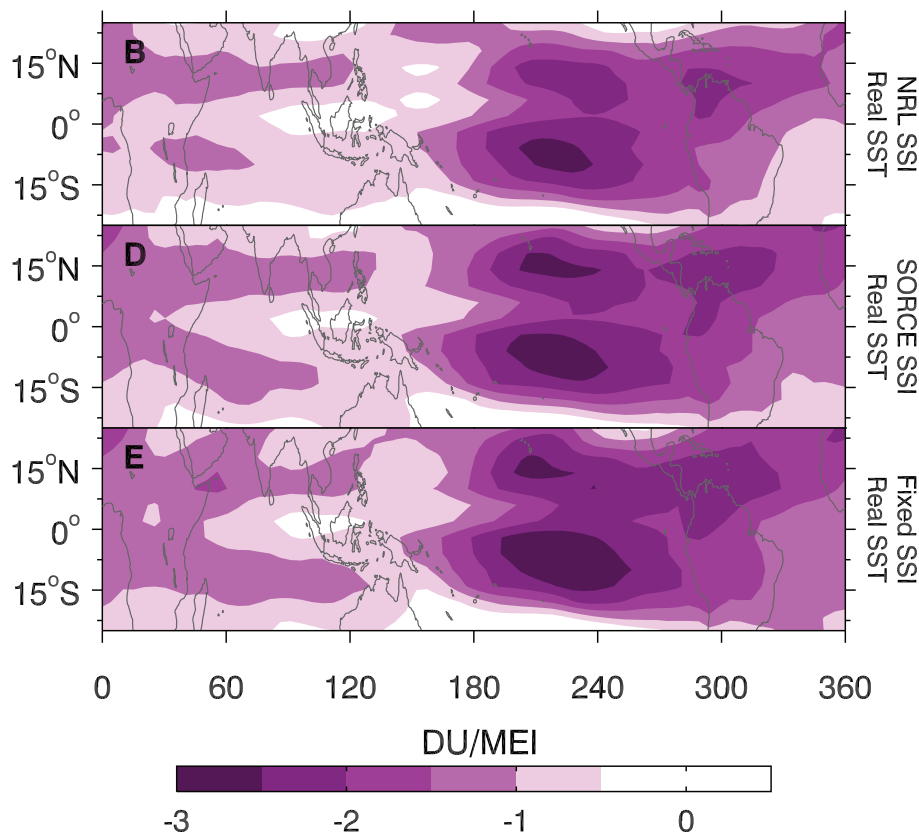


Fig. 5. The spatial pattern of the time-averaged regressed coefficients $\bar{\epsilon}$ related to ENSO for experiments B, D and E.